Load-carrying Capacity of Self-tapping Lag Screws for Glulam-lightweight Concrete Composite Beams

Hao Du,[a] Xiamin Hu,[a,*] Yuchen Jiang,[b] Chenyu Wei,[a] and Wan Hong [a]

When a lag screw with a large diameter is used as the shear connector in timer-concrete composite beams, the procedure of pre-drilling is required during the construction process. In this paper, a new type of lag screw was proposed to omit the pre-drilling step. To investigate the shear behavior of the self-tapping lag screws for glulam-lightweight concrete composite beams, a total of 18 push-out tests were conducted. Based on the push-out test results, the influences of concrete type, screw diameter, and penetration length of screw into timber on the load-carrying capacity were analyzed in detail. The push-out test results showed that the concrete type had no remarkable effect on the load-carrying capacity. The load-carrying capacity was improved with increased screw diameter and penetration length. In addition, an analytical model for load-carrying capacity of lag screw connectors was proposed based on the push-out test results. By comparisons, it was found that the timber-timber and steel-timber models proposed in Eurocode 5 made very conservative predictions on the load-carrying capacity of lag screws. The results of the analytical method presented in this paper showed a better agreement with the experimental results.

Keywords: Glulam-lightweight concrete composite; Self-tapping lag screw; Push-out test; Load-carrying capacity; Analytical model

Contact information: a: College of Civil Engineering, Nanjing Tech University, Nanjing 211816, China; b: College of Civil Engineering, Taihu University of Wuxi, Wuxi 214064, China;
** Corresponding author: huxm_njtech@163.com*

INTRODUCTION

The timber-concrete composite (TCC) beam represents a new structural element in which reliable shear connectors are used to connect a timber beam with a concrete slab. During its use, the timber beam is mainly in tension, and the concrete slab is subjected to compression. Therefore, the two different materials act together in the TCC beam. The mechanical and physical strengths of both components are utilized efficiently (Balogh *et al*. 2007). The TCC beam has several advantages compared with the traditional timber beam, such as greater load-carrying capacity and bending stiffness, improved sound insulation, and less susceptibility to vibration due to the sufficient composite action (Ceccotti 2002; Lukaszewska *et al*. 2008; Yeoh *et al*. 2011).

The shear behavior of connectors has an important effect on the load-bearing capacity and the bending stiffness of TCC beams (Yeoh *et al*. 2011). Therefore, many experimental tests were conducted to investigate the shear performance of dowel-type connectors (He *et al*. 2016). Dias (2005) conducted push-out tests on the dowel-type connectors; the test results showed that the material properties (timber and concrete) and the shape of the connector had an important effect on the load-carrying capacity. Ahmadi and Saka (1993) and Gelfi and Giuriani (1999) studied the effect of penetration depth on

the shear strength of nail and dowel connectors, respectively. The test results showed that the increase of penetration depth had no obvious effect on the load-carrying capacity and stiffness when the ratio between the penetration length and the diameter was increased to a certain value. Fragiacomo *et al*. (2007) conducted experimental tests on the shear stud connectors. A comparison was made between the specimens using normal concrete and lightweight concrete, and their test results showed that the concrete type had no obvious effect on the short-term and long-term performance of the connectors. Deam *et al*. (2008) and Jiang *et al*. (2016) performed push-out tests on coach screw connectors in TCC beams, and the test results showed that the shear performance of screw connectors was mainly influenced by the bearing area. The embedment strength of dowel-type connectors and the bending stiffness of the timber were investigated (Sawata and Yasumura 2002; Gaff *et al*. 2015). Khorsandnia *et al*. (2012) conducted push-out tests on three types of shear connectors (normal screw, specific fastening screw (SFS), and bird-mouth). Analytical models for these connectors were proposed, which can be used in nonlinear finite element models of TCC beams. In addition, some other researchers proposed nonlinear finite element models to analyze the shear behavior of connectors (Dias 2005; Junior and Molina 2010; Oudjene *et al*. 2013).

Thus far, there have been several theoretical methods for determining the load-carrying capacity of dowel-type connectors. The standard EN 1995-1-1 (2014) suggested the calculation formulas for the load-carrying capacity of nails, bolts, dowels, and screws in timber-timber joints and in timber-steel joints. Giuriani *et al*. (2002) presented a calculation model to estimate the load-carrying capacity of stud connectors in timber-concrete joints. It was suggested in this model that the ultimate bearing capacity was obtained when the stud connectors failed with two plastic hinges. Dias *et al*. (2007) evaluated three different analytical models for the load-carrying capacity of dowel connectors. These analytical models were different in the approach used to simulate concrete: elastic-perfectly plastic, linear-elastic, and linear-elastic with crushing. In addition, Xie *et al*. (2017) proposed the models for predicting the load-carrying capacity of a stud-groove connector in glulam-concrete composite beams and verified the analytical methods *via* the push-out test results.

In this paper, a new type of lag screw is proposed to avoid the requirement of pre-drilling. To investigate the shear behavior of the self-tapping lag screws, a total of 18 push-out tests are conducted. Based on the push-out test results, the influences of concrete type, screw diameter, and penetration length of screw into timber on the load-carrying capacity were analyzed in detail. In addition, an analytical method for calculating the load-carrying capacity of the lag screws is presented in this paper.

EXPERIMENTAL

Materials

The glulam used in this test was made of Douglas fir. According to the test method from GB/T 1931 (2009), five specimens with dimensions of 20 mm × 20 mm × 20 mm were tested to obtain the density of the glulam. The density mean value was 536 kg/m^3, and the moisture content was 12.28%. The compression elasticity modulus, compression strength parallel to grain and embedment strength parallel to grain were tested based on GB/T 50329 (2012). The mean compression elasticity modulus of the glulam was 10,680 N/mm^2. The compression strength parallel to grain was 43.4 N/mm^2,

and the embedment strength parallel to grain was 39.2 N/mm^2. For each concrete type, compression tests on three 150 mm cubes were performed. The average compressive strength was 29.4 N/mm^2 and 29.2 N/mm^2 for lightweight concrete and normal concrete, respectively. The yield strength and ultimate tensile strength of the lag screw measured from material tests were 553.9 N/mm^2 and 678.8 N/mm^2, respectively.

Table 1 summarizes the withdrawal capacity of the lag screws with different nominal diameters and penetration lengths in timber. The withdrawal capacity of lag screws was tested according to the standard EN 1382 (2000). According to EN 1995-1-1 (2014), the withdrawal resistance of screw connectors at an angle to grain can be estimated as follows,

$$F_{ax,\alpha} = \frac{n_{\text{ef}} f_{ax} d l_{\text{ef}} k_{\text{d}}}{1.2\cos^2\alpha + \sin^2\alpha} \quad (1)$$

where n_{ef} is the effective number of screws, d is the outer diameter of the threaded part (mm), l_{ef} is the penetration length of the screw (mm), k_{d} is a factor that can be determined as minimum (d/8, 1), α is the angle between the screw and the direction of grain (°), and f_{ax} is the withdrawal strength perpendicular to the grain (N/mm^2). It can be defined as follows,

$$f_{ax} = 0.52 d^{-0.5} l_{\text{ef}}{}^{-0.1} \rho^{0.8} \quad (2)$$

where ρ is the density of timber (kg/m^3).

The axial withdrawal resistance of lag screws perpendicular to the grain can be calculated by Eq. 3 based on the model proposed by Morrison, Hershfield, Burgess, and Huggins (MHBH), and this model was verified by the previously published test results (Kennedy *et al*. 2014).

$$F_{ax} = 110 d^{0.75} l_{\text{ef}} \rho^{1.5} \quad (3)$$

The comparison between the experimental results and the theoretical results obtained from EN 1995-1-1 (2014) and the MHBH's model are shown in Table 1. It was found that the model from EN 1995-1-1 (2014) makes a conservative prediction on the axial withdrawal resistance of lag screws. In addition, the values determined with Eq. 3 were in good agreement with the test results.

Table 1. Axial Withdrawal Capacity of the Lag Screws

Test Series	d (mm)	l_{ef} (mm)	Number of Samples	Axial Withdrawal Capacity F_{ax}		F_{EC5} (kN)	F_{EC5} / F_{ax}	F_{MHBH} (kN)	F_{MHBH} / F_{ax}
				Average (kN)	Coefficient of Variation (%)				
12-100	12	100	6	26.9	6.6	17.4	0.64	28.1	1.04
12-80	12	80	6	21.7	6.1	14.2	0.65	22.5	1.03
12-60	12	60	6	18.2	7.8	11.0	0.60	16.8	0.92
14-100	14	100	6	29.9	8.9	18.8	0.62	31.5	1.05
10-100	10	100	6	24.9	7.1	15.9	0.64	24.5	0.98
Average							0.63		1.01
Coefficient of Variation (%)							2.8		4.8
Note: d is the nominal diameter, l_{ef} is the penetration length in timber, F_{EC5} is the predicted value based on Eurocode 5, and F_{MHBH} is the predicted value based on the MHBH's model.									

Self-tapping lag screw

Generally, when lag screws with a large diameter are used as the shear connectors in TCC beams, the procedure of pre-drilling is required during the construction process. In this paper, a new type of lag screw was proposed to render pre-drilling unnecessary. As shown in Fig. 1, the self-tapping lag screw was successfully drilled into timber. However, the normal lag screw failed to be drilled into the timber without pre-drilling, due to the splitting failure of the timber. Figure 2 illustrates that the self-tapping lag screw consists of six parts: drill, chip storage, thread, collar, screw rod, and hexagon head. The drill located at the end of the lag screw takes full advantage of sharp metal edges to cut timber and guides the screw rod into the timber. The chip storage is used to stack and compact timber chips. The threaded part makes use of the input torque to provide the screw with the feeding force and finally achieves the function of self-tapping. Moreover, the collar is designed to limit the embedded depth of the screw into timber.

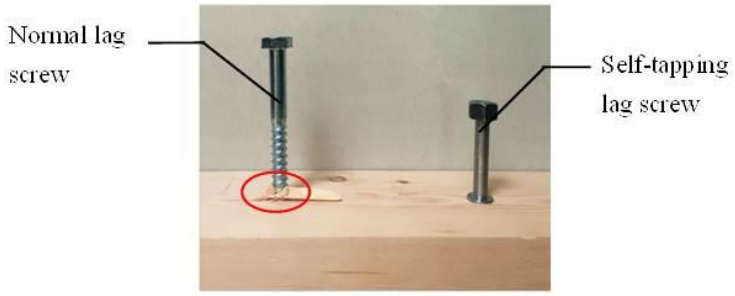

Fig. 1. Comparison between the normal lag screw and self-tapping lag screw

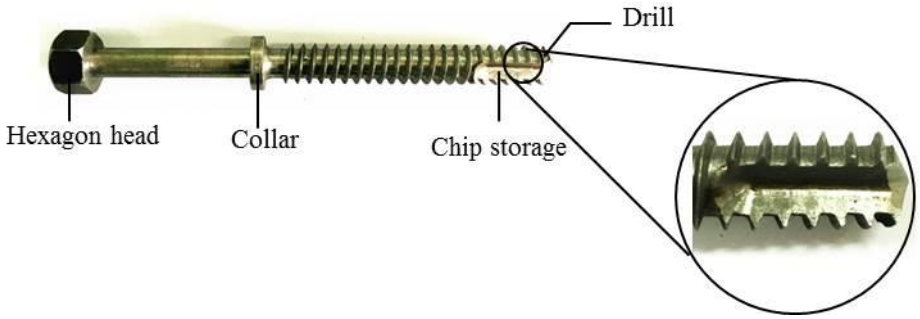

Fig. 2. Details of the self-tapping lag screw

Push-out Specimens

To investigate the shear behavior of the self-tapping lag screw in lightweight concrete, six groups of push-out specimens were designed. The main parameters include concrete type, screw diameter, and penetration depth in timber, and each group consisted of the same three specimens. Table 2 illustrates the parameters of the push-out specimens. In this experiment, the push-out specimens were composed of one 180 mm × 300 mm × 400 mm central timber member, two 80 mm × 400 mm × 400 mm concrete slabs, and two self-tapping lag screws per side. The concrete slab was reinforced with a steel mesh using 8 mm rebar spaced at 150 mm in two directions. The self-tapping lag screws had depths inside the concrete of 60 mm. The details of the push-out specimens are shown in Fig. 3.

Table 2. Test Parameters of Push-out Specimens

Test Series	Concrete Class	Screw Diameter (mm)	Penetration Length (mm)	Screw Length (mm)
NC-12-100	C30	12	100	160
LC-12-100	LC30	12	100	160
LC-14-100	LC30	14	100	160
LC-10-100	LC30	10	100	160
LC-12-80	LC30	12	80	140
LC-12-60	LC30	12	60	120

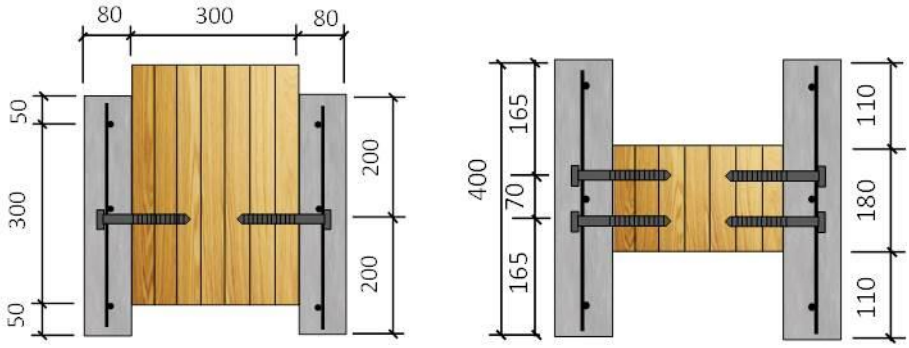

Fig. 3. Details of push-out specimen (mm): a) front view of specimen, and b) top view of specimen

Methods

Test setup and loading procedure

Both the test set-up and the lay-out of the displacement measurements are shown in Fig. 4a. The push-out specimens were loaded using a 200 kN testing machine (MTS Systems Corporation, Shenzhen, China).

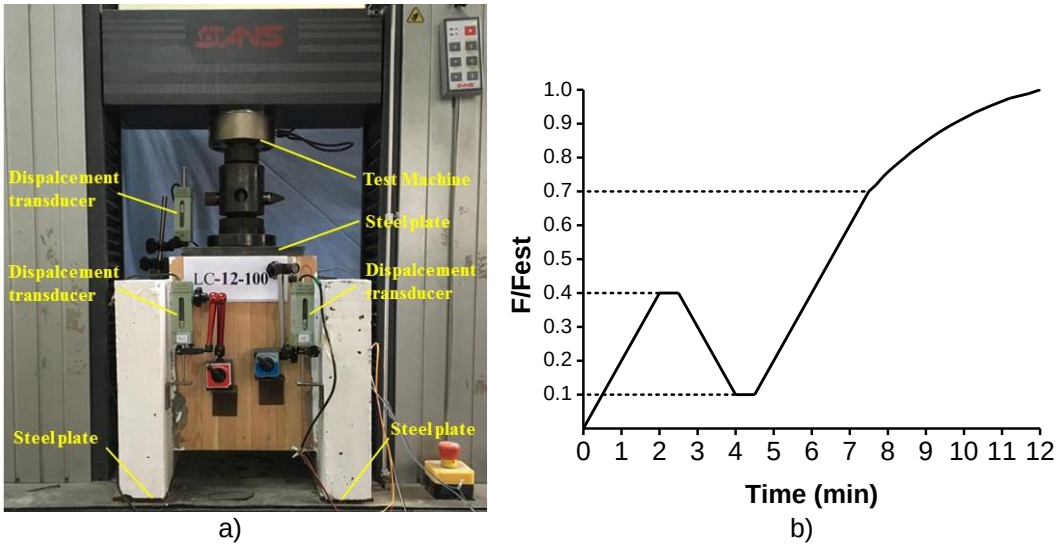

Fig. 4. Test setup: a) View of test setup, and b) Loading procedure

To measure the relative displacement between the concrete slab and the glulam member during the loading process, two displacement transducers were placed, one at each side of the middle specimens, and a displacement meter was installed at the top of the specimens. In addition, a steel plate was placed on the top of the glulam member to distribute the applied force from the test machine.

The implemented loading procedure of all push-out specimens was based on CEN EN 26891 (2001) (Fig. 4b). In the first step, the load was increased to almost 40% of the estimated maximum load (F_{est}) within 2 min. The load was maintained at this level for approximately 30 s. Subsequently, the load was reduced to 0.1 F_{est} within 90 s and maintained at this level for approximately 30 s. Next, the load was increased to almost 0.7 F_{est} in 3 min. Finally, further load was implemented with a displacement control mode until failure of the specimen.

RESULTS AND DISCUSSION

Test Results

All of the specimens were loaded to failure. The ultimate strength F_{max} and the slip modulus K_s of timber-concrete joints were the most important parameters for the design of the timber-concrete composite structures, and the main experimental results are shown in Table 3.

Table 3. Strength and Failure Mode of Push-out Specimens

Specimens	Ultimate Load F_{max} (per screw)			Slip Modulus K_s (per screw)		
	Value (kN)	Average (kN)	COV (%)	Value (kN/mm)	Average (kN/mm)	COV (%)
NC-12-100-1	28.06	29.05	3.7	7.47	6.97	7.0
NC-12-100-2	28.88			6.95		
NC-12-100-3	30.20			6.49		
LC-12-100-1	30.02	28.51	7.2	6.85	6.36	8.7
LC-12-100-2	26.17			6.47		
LC-12-100-3	29.35			5.76		
LC-14-100-1	32.84	32.24	2.0	8.89	8.41	5.3
LC-14-100-2	32.32			8.31		
LC-14-100-3	31.57			8.02		
LC-10-100-1	22.08	21.32	10.5	4.03	4.24	6.9
LC-10-100-2	18.81			4.11		
LC-10-100-3	23.08			4.57		
LC-12-80-1	25.94	26.61	7.9	5.96	5.91	7.4
LC-12-80-2	28.97			6.31		
LC-12-80-3	24.91			5.45		
LC-12-60-1	19.23	18.75	9.8	4.19	4.68	10.1
LC-12-60-2	16.48			4.72		
LC-12-60-3	20.30			5.13		
Note: COV is the coefficient of variation						

In the initial loading stage no visible relative slip was observed due to the bond between the glulam member and the concrete slab. With an increased load, small relative slip was observed and a hissing noise was heard at the interface between the glulam member and the concrete slab. It was observed that the bond at the interface gradually

disappeared. When the load approached 0.6 F_{max}, some horizontal cracks in the concrete slab were observed at the position of the lag screws (Fig. 5a) because the screws were strong enough to cause damage to the concrete members. When the applied load reached its peak, two plastic hinges were formed in the screws, with one at the interface and the other inside the glulam member. Moreover, these events were usually accompanied by the compressive deformation of the glulam around the lag screw (Fig. 5b). It should be noted that the penetration length of the lag screw into timber was comparatively long to allow for the formation of the plastic hinge inside the glulam member.

a) b)

Fig. 5. Test phenomena and failure mode of push-out specimens: a) horizontal crack on the concrete slab, and b) compressive deformation of the glulam and bending deformation of the lag screw

The relationships between shear force and relative slip at the glulam-concrete interface for all push-out specimens are shown in Fig. 6. The load-slip curves for all the test specimens can be approximately divided into two stages: a linear stage and a non-linear stage. As shown in Fig. 6, the linear part had the characteristic of a relatively bigger slope and a smaller slip (< 3 mm). The lag screw connectors had a larger shear stiffness in this stage. While most of the load-slip response was non-linear, the slip increased in spite of the slow load increase, and the stiffness at this stage was lower and continuously decreased. Overall, the lag screw in glulam-lightweight concrete joints had a ductile behavior due to the compressive deformation of the glulam around the screw and the bending deformation of the screw.

Discussion

Based on the push-out test results (Table 3 and Fig. 6), the influences of concrete type, screw diameter, and penetration length of screw into timber on the load-carrying capacity were obtained as follows:

(1) The average load-carrying capacity of the lag screw was 29.05 and 28.51 kN for the test series NC-12-100 and LC-12-100, respectively. The test results indicated that when the compressive strength of normal concrete and lightweight concrete was approximately equal, the concrete type had no remarkable effect on the load-carrying capacity of the lag screw.

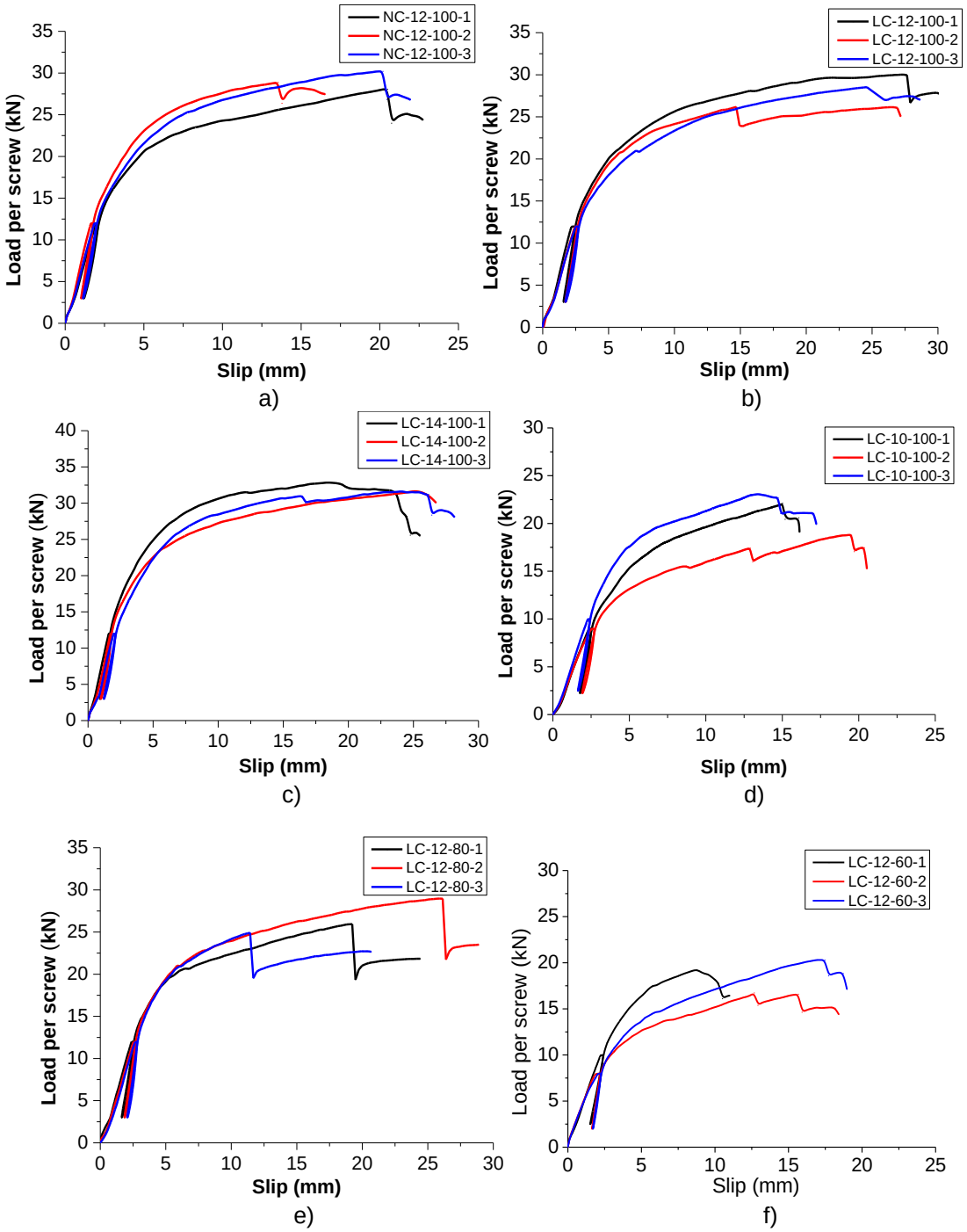

Fig. 6. Load-slip curves for all push-out specimens: a) NC-12-100 test series, b) LC-12-100 test series, c) LC-14-100 test series, d) LC-10-100 test series, e) LC-12-80 test series, and f) LC-12-60 test series

(2) The load-carrying capacity of the lag screws with nominal diameters of 12 and 14 mm was increased 33.7% and 51.2% over that of the lag screw with the diameter of 10 mm, respectively. It was concluded that the lag screw diameter had a remarkable effect on the load-carrying capacity, and the load-carrying capacity improved with increased screw diameter due to the improvement of axial withdrawal capacity and yield moment of the screw connectors.

(3) For the lag screws with penetration lengths of 80 and 100 mm, the load-carrying capacity increased 41.9% and 52.1% over that of the lag screw with the penetration length of 60 mm, respectively. It was found that the load-carrying capacity was improved with increased penetration length. However, when the ratio between the penetration length and the screw diameter increased to a certain value, the load-carrying capacity was not considerably improved. This was because the contribution of the rope effect to the load-carrying capacity should be limited to 100% of the yield strength of the screw connectors according to EN 1995-1-1 (2014).

ANALYTICAL METHODS FOR CALCULATING LOAD-CARRYING CAPACITY

Existing Calculation Methods

In most of the timber standards, the theoretical methods to estimate the load-carrying capacity of shear connectors in timber-timber and timber-steel joints are usually derived based on the Johansen's yield model. In this model, the load-carrying capacity depends on the resistance of the timber and the yield strength of the fastener (Johansen 1949). It is assumed that the bending of the connector and the embedding behavior are both plastic.

If the concrete behavior is also assumed as elastic-plastic, the timber-timber model can be used to estimate the load-carrying capacity of timber-concrete joints. For the failure mode with two plastic hinges in the screw, the calculation method to estimate the load-carrying capacity was proposed in EN 1995-1-1 (2014), as shown in Eq. 4,

$$F_{\mathrm{u,\,t\text{-}t}} = \sqrt{\frac{2\beta}{1+\beta}}\sqrt{2M_{\mathrm{y}} f_{\mathrm{h}} d} + \frac{F_{ax}}{4} \quad (4)$$

where F_{u} is the load-carrying capacity per fastener, f_{h} is the characteristic embedment strength in the timber member (N/mm^2), d is the fastener diameter (mm), $\beta = f_{\mathrm{c}} / f_{\mathrm{h}}$, f_{c} is the characteristic embedment strength in concrete member (N/mm^2), M_{y} is the characteristic fastener yield moment, and F_{ax} is the characteristic axial withdrawal capacity of the fastener.

If the concrete is supposed to be completely rigid, the timber-steel model proposed in EN 1995-1-1 (2014) can be used to predict the load-carrying capacity. When the failure mode is two plastic hinges in the screw, the load-carrying capacity can be determined with Eq. 5:

$$F_{\mathrm{u.\,s\text{-}t}} = \sqrt{4M_{\mathrm{y}} f_{\mathrm{h}} d} + \frac{F_{ax}}{4} \quad (5)$$

The right hand side of Eqs. 4 and 5 was derived based on the Johansen's yield model and it mainly depends on the resistance of the timber around the screw and the bending bearing capacity of the connector. The second part, $F_{\mathrm{ax}}/4$, is to consider the contribution of the rope effect to the load-carrying capacity, which should be limited to 100% of the load-carrying capacity calculated by the Johansen's yield model. The withdrawal capacity for screw connectors was determined with Eq. 1 based on the EN 1995-1-1 (2014) standard.

Calculation Proposal

In this paper it has been assumed that the concrete was completely rigid and the fixity of the lag screw in concrete was perfect. In this case, the mechanical model of the failure mode with two plastic hinges in the screw is presented in Fig. 7. The yield moment of the lag screw is expressed as,

$$M_{\mathrm{y}} = \frac{f_{\mathrm{h}} d x^2}{4} \tag{6}$$

where x is the distance (mm) between two plastic hinges.

Shear force in the lag screw between the timber beam and the concrete slab was calculated by Eq. 7:

$$V_{\mathrm{u}} = f_{\mathrm{h}} d x \tag{7}$$

Substituting x from Eq. 6 into Eq. 7, the shear force V_{u} is expressed as Eq. 8:

$$V_{\mathrm{u}} = 2\sqrt{f_{\mathrm{h}} d M_{\mathrm{y}}} \tag{8}$$

The load-carrying capacity of the lag screw can be determined by,

$$F_{\mathrm{u}} = V_{\mathrm{u}} \sin\alpha + F_{\mathrm{ax}} \cos\alpha \tag{9}$$

where α is the angle between the screw and the interface. Based on the push-out test results, the angle α was 60° to 70°. In this paper, the angle α was taken as 70° in the conservative way. Substituting Eq. 3 and Eq. 8 into Eq. 9, the load-carrying capacity $F_{\mathrm{u,ct}}$ was derived:

$$F_{\mathrm{u,\,ct}} = 1.88\sqrt{f_{\mathrm{h}} d M_{\mathrm{y}}} + 37.62 d^{0.75} l_{\mathrm{ef}} \rho^{1.5} \tag{10}$$

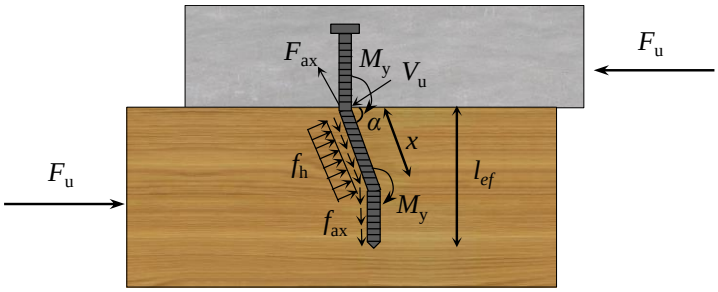

Fig. 7. Mechanical model of the failure mode with two plastic hinges in the screw

Comparison between Experimental and Theoretical Results

The theoretical results from different models were compared with the push-out test results in this paper and the previously published test results (Deam *et al*. 2008; Oudjene *et al*. 2013; Jiang *et al*. 2016), as shown in Table 4. It can be concluded that the timber-timber and steel-timber calculation models proposed in EN 1995-1-1 (2014) make a conservative prediction on the load-carrying capacity of lag screw connectors. Dias *et al.* (2004) considered that the post-yielding strength of the screws accounted for over 50% of the load-carrying capacity. In addition, Jiang *et al.* (2017) held that the calculation models in EN 1995-1-1 (2014) underestimated the load-carrying capacity of the screw connectors, due to neglecting some rope effects.

Table 4. Comparison between the Experimental Results and the Calculated Results Obtained from Different Models

References	Specimen	F_u	$F_{u,t\text{-}t}$	$F_{u,s\text{-}t}$	$F_{u,ct}$	$F_{u,t\text{-}t}/F_u$	$F_{u,s\text{-}t}/F_u$	$F_{u,ct}/F_u$
This paper	NC-12-100-1	28.06	14.62	20.11	24.81	0.52	0.72	0.88
	NC-12-100-2	28.88	14.62	20.11	24.81	0.51	0.70	0.86
	NC-12-100-3	30.20	14.62	20.11	24.81	0.48	0.67	0.82
	LC-12-100-1	30.02	14.64	20.11	24.81	0.49	0.67	0.83
	LC-12-100-2	26.17	14.64	20.11	24.81	0.56	0.77	0.95
	LC-12-100-3	29.35	14.64	20.11	24.81	0.50	0.69	0.85
	LC-14-100-1	32.84	18.27	25.49	30.80	0.56	0.78	0.94
	LC-14-100-2	32.32	18.27	25.49	30.80	0.57	0.79	0.95
	LC-14-100-3	31.57	18.27	25.49	30.80	0.58	0.81	0.98
	LC-10-100-1	22.08	11.38	15.32	19.37	0.52	0.69	0.88
	LC-10-100-2	18.81	11.38	15.32	19.37	0.61	0.81	1.03
	LC-10-100-3	23.08	11.38	15.32	19.37	0.49	0.66	0.84
	LC-12-80-1	25.94	14.02	19.98	23.47	0.54	0.77	0.90
	LC-12-80-2	28.97	14.02	19.98	23.47	0.48	0.69	0.81
	LC-12-80-3	24.91	14.02	19.98	23.47	0.56	0.80	0.94
	LC-12-60-1	19.23	13.03	18.50	20.87	0.68	0.96	1.09
	LC-12-60-2	16.48	13.03	18.50	20.87	0.79	1.12	1.27
	LC-12-60-3	20.30	13.03	18.50	20.87	0.64	0.91	1.03
Deam *et al.* 2008	Spec.13	21.50	12.85	16.44	23.10	0.60	0.76	1.07
	Spec.14	34.20	18.97	24.99	33.43	0.55	0.73	0.98
Oudjene *et al.* 2013	Spec.1	17.09	7.27	9.33	11.46	0.43	0.55	0.67
	Spec.2	14.98	7.31	9.33	11.46	0.49	0.62	0.77
	Spec.3	17.70	7.25	9.33	11.46	0.41	0.53	0.65
Jiang *et al.* 2016	S-1-1	16.75	8.54	11.12	13.51	0.51	0.66	0.81
	S-1-2	15.50	8.54	11.12	13.51	0.55	0.72	0.87
	S-1-3	15.50	8.54	11.12	13.51	0.55	0.72	0.87
	S-2-1	16.00	8.07	10.65	12.51	0.50	0.67	0.78
	S-2-2	14.50	8.07	10.65	12.51	0.56	0.73	0.86
	S-2-3	14.00	8.07	10.65	12.51	0.58	0.76	0.89
	S-4-1	18.00	10.95	14.46	17.26	0.61	0.80	0.96
	S-4-2	18.00	10.95	14.46	17.26	0.61	0.80	0.96
	S-4-3	18.00	10.95	14.46	17.26	0.61	0.80	0.96
	S-5-1	13.00	10.44	13.94	16.10	0.80	1.07	1.24
	S-5-2	15.00	10.44	13.94	16.10	0.70	0.93	1.07
	S-5-3	13.50	10.44	13.94	16.10	0.77	1.03	1.19
	S-7-1	12.00	6.40	8.18	10.12	0.53	0.68	0.84
	S-7-2	12.00	6.40	8.18	10.12	0.53	0.68	0.84
	S-7-3	13.00	6.40	8.18	10.12	0.49	0.63	0.78
	S-8-1	12.00	6.24	8.18	10.12	0.52	0.68	0.84
	S-8-2	12.00	6.24	8.18	10.12	0.52	0.68	0.84
	S-8-3	11.00	6.24	8.18	10.12	0.57	0.74	0.92
	S-9-1	15.00	6.63	8.18	10.12	0.44	0.55	0.67
	S-9-2	13.50	6.63	8.18	10.12	0.49	0.61	0.75
	S-9-3	13.00	6.63	8.18	10.12	0.51	0.63	0.78
	S-10-1	18.50	10.95	14.46	17.26	0.59	0.78	0.93
	S-10-2	19.00	10.95	14.46	17.26	0.58	0.76	0.91
	S-10-3	17.50	10.95	14.46	17.26	0.63	0.83	0.99
Average						0.56	0.75	0.91
Coefficient of Variation (%)						15	17	15

Note: F_u is experimental results, $F_{u,t\text{-}t}$ is calculated from timber-timber model, $F_{u,s\text{-}t}$ is calculated results from steel-timber model, and $F_{u,ct}$ is calculated results based on the proposed model.

According to the theoretical results from EN 1995-1-1 (2014), approximately 24% of the load-carrying capacity came from the contribution of the rope effects. In addition, the comparisons showed that the predictions based on the model proposed in this paper were in better agreement with the experimental results.

CONCLUSIONS

In this paper, a new type of lag screw was proposed to get around the need for pre-drilling. To investigate the shear behavior of the self-tapping lag screws for glulam-lightweight concrete composite beams, a total of 18 push-out tests were conducted. According to the experimental and theoretical study performed in this paper, the following conclusions were drawn:

1. The analytical method from Eurocode 5 made a conservative prediction on the axial withdrawal resistance of the lag screws. In addition, the values determined with the MHBH's model were in good agreement with the experimental results.
2. The lag screw in glulam-lightweight concrete joints had a ductile behavior, due to the compressive deformation of the glulam around the screw and the bending deformation of the screw. The failure mode with two plastic hinges in lag screw was observed in the push-out tests.
3. The concrete type had no remarkable effect on the load-carrying capacity of the lag screw when the compressive strength of lightweight concrete and normal concrete was approximately equal. The load-carrying capacity improved with increased screw diameter and penetration length. However, when the ration between the penetration length and the screw diameter increased to a certain value, the load-carrying capacity was not considerably improved.
4. The timber-timber and steel-timber models proposed in Eurocode 5 make a very conservative prediction on the load-carrying capacity of lag screws. The predictions based on the model presented in this paper showed a better agreement with the experimental results.

ACKNOWLEDGMENTS

The research was supported by the National Natural Science Foundation of China (Nos. 51678295 and 51478220), and the Research Innovation Program for College Graduates of Jiangsu Province (No. KYCX17_0914). The authors also thank Associate Prof. Hongqi Yang for revising and proofreading this manuscript.

REFERENCES CITED

Ahmadi, B. H., and Saka, M. P. (1993). "Behavior of composite timber-concrete floors," *Journal of Structural Engineering* 119(11), 3111-3130. DOI: 10.1061/(ASE)0733-9445(1993)119:11(3111)

Balogh, J., Wieligmann, M., Gutkowski, R., and Haller, P. (2007). "Stress–strain behavior of connections for partially composite wood–concrete floors and deck systems," in: *2nd Material Specialty Conference of the Canadian Society for Civil Engineering*, Vol. 6, Montreal, Canada, pp. 505-513.

Ceccotti, A. (2002). "Composite concrete–timber structures," *Progress in Structural Engineering and Material* 4(3), 264–275.

CEN EN 26891 (2000). "Timber structures - Joints made with mechanical fasteners - General principles for the determination of strength and deformation characteristics," European Committee for Standardization, Brussels, Belgium.

Deam, B. L., Fragiacomo, M., and Buchanan, A. H. (2008). "Connections for composite concrete slab and LVL flooring systems," *Materials and Structures* 41(3), 495-507. DOI: 10.1617/s11527-007-9261-x

Dias, A. M. P. G. (2005). *Mechanical Behaviour of Timber–Concrete Joints*, Ph.D. Thesis, University of Coimbra, Coimbra, Portugal.

Dias, A. M. P. G., Cruz, H. M. P., Lopes, S., and Kuilen, J. W. G. V. D. (2004). "Experimental shear-friction tests on dowel type fastener timber-concrete joints," in: *Proceedings of the 8th WCTE*, Lahti, Finland.

Dias, A. M. P. G., Lopes, S. M. R., Kuilen, J. W. G. V. D., and Cruz, H. M. P. (2007). "Load-carrying capacity of timber-concrete joints with dowel-type fasteners," *Journal of Structural Engineering* 133(5), 720-727. DOI: 10.1061/(ASCE)0733-9445(2007)133:5(720)

EN 1382 (2000). "Timber structures - Test methods - Withdrawal capacity of timber fasteners," European Committee for Standardization, Brussels, Belgium.

EN 1995-1-1 (2014). "Eurocode 5: Design of timber structures - Part 1-1: General rules and rules for buildings," European Committee for Standardization, Brussels, Belgium.

Fragiacomo, M., Amadio, C., and Macorin, L. (2007). "Short and long term performance of the Tecnaria stud connector for timber-concrete composite beams," *Materials and Structures* 40(10), 1013-1026. DOI: 10.1617/s11527-006-9200-2

Gaff, M., Gašparík, M., Borůvka, V., Haviarová, E. (2015). "Stress simulation in layered wood-based materials under mechanical loading," *Materials and Design* 87, 1065-1071. DOI: 10.1016/j.matdes.2015.08.128

GB/T 1931 (2009). "Method for determination of the moisture content of wood," Standardization Administration of China, Beijing, China.

GB/T 50329 (2012). "Standard for methods testing of timber structures" Standardization Administration of China, Beijing, China.

Gelfi, P., and Giuriani, E. (1999). "Behaviour of stud connectors in wood-concrete composite beams," in: *Proceedings of the Structural Studies, Repair and Maintenance of Historical Buildings VI: 6th International Conference*, Wit Press, Dresden, Germany, pp. 565–578.

Giuriani, E., Marini, A., and Gelfi, P. (2002). "Stud shear connection design for composite concrete slab and wood beams," *Journal of Structural Engineering* 128(12), 1544-1550. DOI: 10.1061/(ASCE)0733-9445(2002)128:12(1544)

He, G., Xie, L., Wang, A., Yi, J., Peng, L., Chen, Z., Gustafsson, P. J., and Crocetti, R. (2016). "Shear behavior study on timber-concrete composite structures with bolts," *BioResources* 11(4), 9205-9218. DOI: 10.15376/biores.11.4.9205-9218

Jiang, Y., Hong, W., Hu, X., Crocetti, R., Wang, L., and Sun, W. (2017). "Early-age performance of lag screw shear connections for glulam-lightweight concrete

composite beams," *Construction and Building Materials* 151, 36-42. DOI: 10.1016/j.conbuildmat.2017.06.063

Jiang, Y., Hu, X., Cao, X., Hong, W., and Zhang, B. (2016). "Experimental study on push-out tests of screw connectors for glulam-concrete composite beams," *Journal of Nanjing Tech University (Natural Science Edition)* 38(5), 74-80 (in Chinese). DOI: 10.3969/j.issn.1671-7627.2016.05.012

Johansen, K. W. (1949). "Theory of timber connections," *International Association for Bridge and Structural Engineering* 9, 249–262.

Junior, C. C., and Molina, J. C. (2010). "Numerical modeling strategy for analyzing the behaviour of shear connectors in wood-concrete composite systems," in: *World Conference on Timber Engineering*, Riva Del Garda, Italy.

Kennedy, S., Salenikovich, A., Munoz, W., and Mohammad, M. (2014). "Design equation for withdrawal resistance of threaded fasteners in the Canadian timber design code," *World Conference on Timber Engineering*, Québec, Canada.

Khorsandnia, N., Valipour, H. R., and Crews, K. (2012). "Experimental and analytical investigation of short-term behaviour of LVL-concrete composite connections and beams," *Construction and Building Material* 37(12), 229-238. DOI: 10.1016/j.conbuildmat.2012.07.022

Lukaszewska, E., Johnsson, H., and Fragiacomo, M. (2008). "Performance of connections for prefabricated timber-concrete composite floors," *Materials and Structures* 41(9), 1533-1550. DOI: 10.1617/s11527-007-9346-6

Oudjene, M., Meghlat, E. M., Ait-Aider, H., and Batoz, J. L. (2013). "Non-linear finite element modelling of the structural behaviour of screwed timber-to-concrete composite connections," *Composite Structures* 102(4), 20-28. DOI: 10.1016/j.compstruct.2013.02.007

Sawata, K., and Yasumura, M. (2002). "Determination of embedding strength of wood for dowel-type fasteners," *Journal of Wood Science* 48, 138-146. DOI:10.1007/bf00767291

Xie, L., He, G., Wang, A., Gustafsson, P. J., Crocetti, R., Chen, L., Li, L., and Xie, W. (2017). "Shear capacity of stud-groove connector in glulam-concrete composite structure," *BioResources* 12(3), 4690-4706. DOI: 10.15376/biores.12.3.4690-4706

Yeoh, D., Fragiacomo, M., Franceschi, M. D., and Boon, K. H. (2011). "State of the art on timber-concrete composite structures: Literature review," *Journal of Structural Engineering* 137(10), 1085-1095. DOI: 10.1061/(ASCE)st.1943-541x.0000353

Article submitted: September 8, 2018; Peer review completed: October 28, 2018; Revised version received: November 9, 2018; Accepted: November 11, 2018; Published: November 14, 2018.
DOI: 10.15376/biores.14.1.166-179